AIChE WILEY InterScience DISCOVER SOMETHING GREAT

Modeling Extraction Separation of Nd(III) and La(III) from Nitrate Media in Hollow-Fiber Modules

Ruey-Shin Juang, Hsiang-Chien Kao, and Pei-Shin Yen
Dept. of Chemical Engineering and Materials Science, Yuan Ze University, Chung-Li 32003, Taiwan

DOI 10.1002/aic.11103
Published online January 29, 2007 in Wiley InterScience (www.interscience.wiley.com).

The use of two microporous hollow-fiber modules for simultaneous extraction and stripping of binary Nd(III) and La(III) from nitrate media with a kerosene solution of 2-ethylhexylphosphonic acid mono-2-ethylhexyl ester (PC88A) to a HNO_3 solution was investigated. Experiments were carried out at different feed pH values (2–6), total metal concentrations (2–24 g-mol/m^3), metal concentration ratios (0.25–4), and dimeric PC88A concentrations (17–137 g-mol/m^3). A kinetic model was presented that takes into account the resistances of diffusion in the aqueous stagnant layer, membrane pore, and organic stagnant layer as well as interfacial reactions. It was shown that the calculated time changes of the feed- and strip-phase metal concentrations were in acceptable agreement with the measured data (standard deviation, 8%). The extraction process was dominated by membrane diffusion under the conditions studied, whereas the stripping process was primarily governed by combined membrane and aqueous strip-layer diffusion. Effective separation of Nd(III) over La(III) by PC88A in such continuous NDSX process could be achieved, mainly by selective stripping, at high feed pH values or low organic PC88A concentrations. © 2007 American Institute of Chemical Engineers *AIChE J,* 53: 561–571, 2007
Keywords: extraction separation, Nd(III) and La(III), PC88A, hollow-fiber modules, mass-transfer mechanisms

Introduction

As a result of the growing demand for high-purity metals, concerns over environmental issues, and the need for lower production costs, selective recovery of metal values from raw and waste resources (ores, sludge, scrap, spent catalysts, etc.) become an important issue. One example is the recovery of rare earth metals such as La(III) and Nd(III) from spent Ni-metal hydride (Ni-MH) secondary batteries.[1,2] The rectangular and circular cylinder-shaped Ni-MH batteries have been treated in the Energy and Resources Laboratories (Industrial Technology Research Institute, Hsinchu, Taiwan). The package of Ni-MH batteries was first dismantled and cut in half crosswise to separate metallic cases from internal battery rolls that consisted of the cathode and anode plus a nylon separator. After washing with water to remove water-soluble components, they were heated in an oven at 600°C for 0.5 h to remove the organic constituents. The solids were ground and sieved as fine powders (<50 mesh) and were then leached by 3 mol/dm^3 HCl (mol is defined as g-mol hereafter) at a solid–liquid ratio of 1:7 for 1 h at 90°C. The leach liquor was treated by successively adding 6 mol/dm^3 NaOH until $Al(OH)_3$ and $Fe(OH)_3$ were completely precipitated. After filtration, the liquor (pH < 2) was extracted with 20 vol % di(2-ethylhexyl)phosphoric acid (D2EHPA) in kerosene.[1,2] The aqueous raffinate contains Ni(II), Co(II), and Mn(II), where the former two metals can be recovered by electrodeposition or other solvent extraction circuits.[2,3] An aqueous solution containing around 3.5 g/dm^3 La(III) and 2.0 g/dm^3 Nd(III) was obtained when the loaded organic phase was further stripped by 1 mol/dm^3 HNO_3.

2-Ethylhexylphosphonic acid mono-2-ethylhexyl ester (PC88A) has shown superior ability for recovery and separation of Nd(III) and La(III) from nitrate media by solvent extraction (SX), compared with other organophosphorus extractants such as

Correspondence concerning this article should be addressed to R.-S. Juang at rsjuang@ce.yzu.edu.tw.

© 2007 American Institute of Chemical Engineers

ID: 3b2server Date: 13/2/07 Time: 07:58 Path: J:/Wiley_Sgml/JOHNWILEY/3B2-Final-Pdfs/Electronic/WEB_PDF/Process/C2AIC#070001

Table 1. Values of Parameters Used for Modeling the NDSX Processes of Binary Nd(III) and La(III) with PC88A at 25°C

Parameter	La(III) System	Nd(III) System	Reference
Extraction constant:			
K_{ex}	2.30×10^{-5}	2.39×10^{-4}	4
k_1	1.2×10^{-6} $m^{5/2}/(mol^{1/2}/s)$	3.3×10^{-7} $m^4/(mol/s)$	4
k_{-1}	7.8×10^{-5} $mol^{1/2}/(m^{1/2}/s)$	2.7×10^{-4} $mol/(m^2/s)$	4
Diffusivity:			
$D_{M,a}$	6.2×10^{-10} m^2/s	5.7×10^{-10} m^2/s	24
$D_{H,a}$	9.3×10^{-9} m^2/s	9.3×10^{-9} m^2/s	24
$D_{(HX)2,o}$	6.3×10^{-10} m^2/s	6.3×10^{-10} m^2/s	25
$D_{MX3,o}$	4.0×10^{-10} m^2/s	4.0×10^{-10} m^2/s	25
Mass transfer coefficient:			
$k_{M,a}$	5.0×10^{-6} m/s	4.7×10^{-6} m/s	This work
$k_{H,a}$	3.1×10^{-5} m/s	3.1×10^{-5} m/s	This work
$k_{(HX)2,o}$	3.9×10^{-6} m/s	3.9×10^{-6} m/s	This work
$k_{MX3,o}$	2.8×10^{-6} m/s	2.8×10^{-6} m/s	This work
$k_{(HX)2,m}$	1.4×10^{-6} m/s	1.4×10^{-6} m/s	This work
$k_{MX3,m}$	8.7×10^{-7} m/s	8.7×10^{-7} m/s	This work

D2EHPA and Cyanex 272.[4] The SX separation of Nd(III) from La(III) with PC88A is not only thermodynamically but also kinetically favorable. However, conventional SX processes are operated in devices such as packed towers and mixer-settlers, which seek to maximize the contact area of two immiscible phases for mass transfer. The intimate mixing that takes place in these devices leads to the formation of stable emulsions or the third phase, thereby inhibiting phase separation and product recovery.[5] Moreover, traditional SX systems avoid using liquids having similar densities, a situation that appears to promote these problems.[6] Additional limitations present in packed towers include the loading requirements and flooding restrictions.

Many of the above-cited shortcomings associated with SX could be minimized or eliminated using the so-called nondispersive solvent extraction (NDSX) in membrane contactors.[7,8] When a microporous membrane is put in contact with a fluid that wets the membrane, the fluid fills the pores of the membrane. If a second immiscible liquid is allowed to contact the membrane, an interfacial contact area is established on that side of the membrane surface. Moreover, because they are simpler to operate than traditional SX units, NDSX processes using hollow fibers are of particular interest because of their versatility. Hollow-fiber modules are connected in series or in parallel, and the length and diameter of fibers and modules can be varied to provide the required contact area. Some researchers believe that this method may be economically comparable to ion exchange and reverse osmosis.[7,8]

In this work, simultaneous extraction and stripping of binary Nd(III) and La(III) from nitrate media with PC88A in two microporous hollow-fiber modules were investigated. One module is the extraction and the other is the stripping, which can actually eliminate the equilibrium limitation and obtain high efficiency.[8,9] Thus, it is highly desirable to systematically examine the performance and mass-transfer characteristics of extraction processes in hollow-fiber modules.[10] Experiments were made at different total metal concentrations (2–24 mol/m^3), metal concentration ratios (0.25–4), pH values (2–6), and PC88A dimer concentrations (17–137 mol/m^3). The separation factors of Nd(III) over La(III) obtained between NDSX and batch SX processes were compared. We will propose a kinetic model to analyze the present NDSX processes based on a good knowledge of the extraction chemistry and the transport properties of relevant geometry.[11–13] The validity of the kinetic model was justified from the predictions of the measured time profiles of metal concentrations in the aqueous feed and strip phases. The mass-transfer mechanisms were determined by comparing the relative resistances of all possible steps including interfacial chemical reactions and diffusion in the aqueous stagnant layer, membrane, and organic stagnant layer.

Modeling of the Mass Transfer

Chemistry of solvent extraction (SX)

According to separate batch experiments,[4] the stoichiometry for the extraction of La(III) and Nd(III) from nitrate solutions with PC88A (HX) dissolved in kerosene can be written as follows:

$$M^{3+} + 3\overline{(HX)_2} \Leftrightarrow \overline{MX_3(HX)_3} + 3H^+ \quad K_{ex,M} \qquad (1)$$

where the overbar refers to the organic phase. The symbol $(HX)_2$ denotes that PC88A mainly exists as the dimers in nonpolar or weak polar solvents such as kerosene.[4,14] The extraction equilibrium constant $K_{ex,M}$ is thus given by

$$K_{ex,M} = \frac{\overline{[MX_3(HX)_3]}[H^+]^3}{[M^{3+}][\overline{(HX)_2}]^3} \qquad (2)$$

Table 1 lists the values of $K_{ex,M}$ for La(III) and Nd(III) at 25°C.

Based on the kinetic studies of batch SX in a constant interface-area stirred cell,[4] the rate of La(III) and Nd(III) extraction with PC88A in kerosene (R_M) can be expressed as a combination of forward (extraction) and backward (stripping) rates:

$$R_{La} = k_{1,La}[La^{3+}][\overline{(HX)_2}]^{1/2} - k_{-1,La}[\overline{LaX_3}][H^+]^{-1/2} \qquad (3)$$

$$R_{Nd} = k_{1,Nd}[Nd^{3+}][\overline{(HX)_2}] - k_{-1,Nd}[\overline{NdX_3}][H^+]^{-1} \qquad (4)$$

The forward rate constants k_1 for La(III) and Nd(III) are obtained to be 1.2×10^{-6} $m^{5/2}/(mol^{1/2}$ s) and 3.3×10^{-7} $m^4/$(mol s), respectively, at 25°C. The backward rate constants k_{-1} for La(III) and Nd(III) are obtained to be 7.8×10^{-5} $mol^{1/2}/(m^{1/2}$ s) and 2.7×10^{-4} $mol/(m^2$ s), respectively.

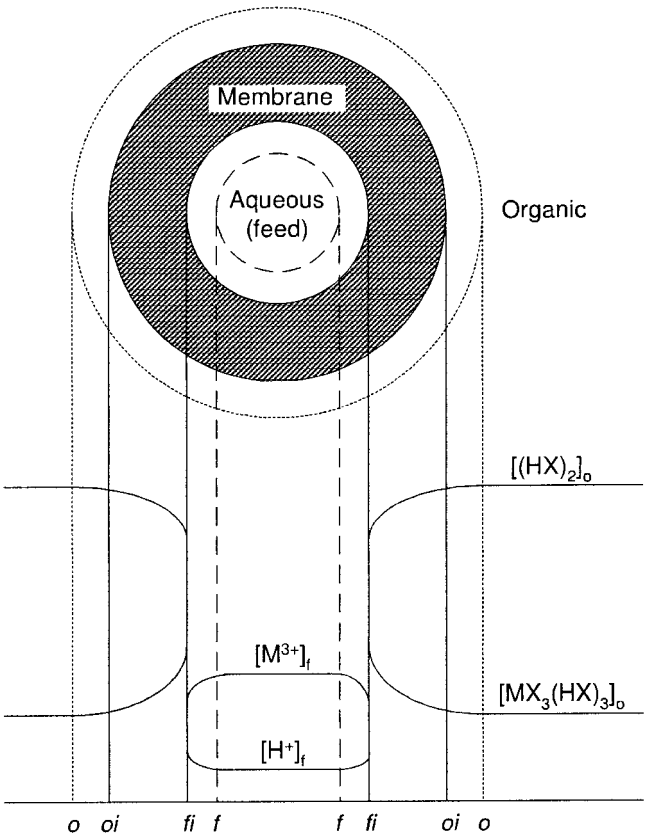

Figure 1. Concentration profiles of reactive species around and within a hollow fiber in the extraction module.

Equations 3 and 4 indicate that the forward rates of La(III) and Nd(III) are comparable but the backward rate of Nd(III) is nearly two orders of magnitude larger than that of La(III). Here, the rate equations for the extraction of La(III) (Eq. 3) and Nd(III) (Eq. 4) cannot lead to the corresponding equilibrium relationships (Eq. 2). This is probably because the extraction reactions take place by a composite mechanism, where the rate equations would change with experimental conditions, such as reactant concentrations, and the rate constants also change.[15]

Mass transfer in the NDSX processes

It was assumed that hydrophobic membranes with a pore size between 10^{-3} and 10^{2} μm are not wetted by water, although hydrocarbons and most organic solvents can wet them.[16] The concentrations of species at both sides of the membrane–organic interface are assumed to be the same because the interface is basically homogeneous as a result of the medium porosity of the membrane. Figure 1 shows the concentration profiles of species in and around a fiber in the extraction module. In this model, metal ions diffuse through the aqueous stagnant layer to the feed–membrane interface where they react with PC88A carrier to form the complex. The complex then diffuses through the membrane and organic stagnant layer to the bulk phase. In the meantime, free PC88A carriers and H^+ diffuse in the reverse direction through the membrane.

From a macroscopic perspective (that is, changes of metal concentrations in the feed and organic phases), the NDSX process is a dynamic one that can be treated using an unsteady mass balance. On the other hand, the transport of metal ions through the membrane (that is, the microscopic process) can be viewed as a steady-state process because the macroscopic process time is longer than the time required for the microscopic process.[17] Therefore, a pseudosteady state is assumed for the present microscopic process at a certain time.[10,11,18] If the diffusion process is described in terms of the mass-transfer coefficient, the following set of flux equations holds:

$$\begin{aligned} J_{M,E} &= k_{M,f}A_i\left([M^{3+}]_f - [M^{3+}]_{fi}\right) = A_i(R_M)_{fi} \\ &= k_{\mathrm{MX_3},m}A_{lm}\left(\overline{[\mathrm{MX_3}]}^m_{fi} - \overline{[\mathrm{MX_3}]}^m_{oi}\right) \\ &= k_{\mathrm{MX_3},o}A_o\left(\overline{[\mathrm{MX_3}]}_{oi} - \overline{[\mathrm{MX_3}]}_o\right) \\ &= \left(\frac{1}{3}\right)k_{H,f}A_i\left([H^+]_{fi} - [H^+]_f\right) \end{aligned} \quad (5)$$

where the superscript m refers to the membrane side adjacent to the aqueous–membrane interface and, for simplicity, MX_3 denotes the complex $MX_3(HX)_3$. A_i, A_{lm}, and A_o are, respectively, the effective contact areas based on the inner, log mean, and outer diameters of the fibers (m^2).

The continuity of the total flux of the carrier in the extraction module is expressed by

$$\begin{aligned} K_{(\mathrm{HX})_2}\left(\overline{[(\mathrm{HX})_2]}_o - \overline{[(\mathrm{HX})_2]}^m_{fi}\right) &= 3K_{\mathrm{LaX_3}}\left(\overline{[\mathrm{LaX_3}]}^m_{fi} - \overline{[\mathrm{LaX_3}]}_o\right) \\ &+ 3K_{\mathrm{NdX_3}}\left(\overline{[\mathrm{NdX_3}]}^m_{fi} - \overline{[\mathrm{NdX_3}]}_o\right) \end{aligned} \quad (6)$$

where K_j refers to the overall mass-transfer coefficient of species j covering the membrane and organic stagnant layer; that is, $(1/K_j) = (1/k_{j,\mathrm{m}}) + (1/k_{j,\mathrm{o}})$. Moreover, the following mass balance for the PC88A carrier holds in the extraction module if the concentration profiles in the membrane and organic stagnant layer are linear[10]

$$\begin{aligned} &\overline{[(\mathrm{HX})_2]}_0 - \overline{[(\mathrm{HX})_2]}_o \\ &\quad = \int\left(\overline{[(\mathrm{HX})_2]} + 3\sum\overline{[\mathrm{MX_3}]}\right)dx \\ &\quad = \left(\frac{1}{2}\right)\left\{\overline{[(\mathrm{HX})_2]}^m_{fi} + 2\overline{[(\mathrm{HX})_2]}^m_{oi} + \overline{[(\mathrm{HX})_2]}_{oi}\right. \\ &\quad \left. + 3\sum\left(\overline{[(\mathrm{MX})_3]}^m_{fi} + 2\overline{[(\mathrm{MX})_3]}^m_{oi} + \overline{[(\mathrm{MX})_3]}_{oi}\right)\right\} \end{aligned} \quad (7)$$

Because it is assumed that the membrane–organic interface is homogeneous, the concentrations of species at this interface are identical; that is, $\overline{[MX_3]}^m_{oi} = \overline{[MX_3]}_{oi}$ and $\overline{[HX_2]}^m_{oi} = \overline{[HX_2]}_{oi}$.

In the stripping module of the NDSX process, the concentration profiles in and around a fiber are shown in Figure 2. The metal complex diffuses through the organic stagnant layer and membrane to the membrane–strip interface, where the complex reacts with H^+ to release metal ions and PC88A is regenerated. Metals then diffuse through the aqueous stagnant layer to the bulk phase. Meanwhile, the regenerated PC88A carriers counterdiffuse through the membrane. In this case, the molar flux of metal in the stripping module ($J_{\mathrm{M,S}}$) can be described by the following equation system:

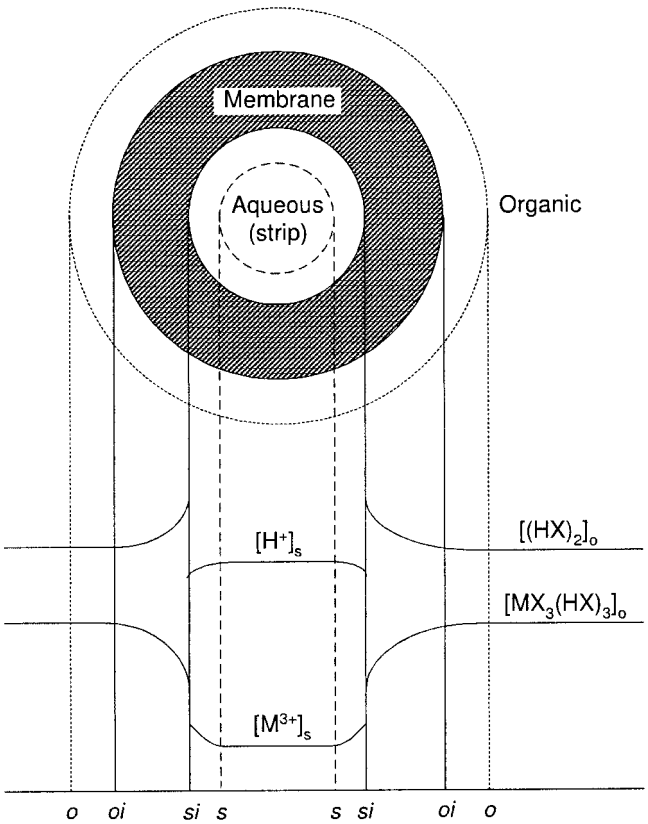

Figure 2. Concentration profiles of reactive species around and within a hollow fiber in the stripping module.

$$J_{M,S} = k_{MX_3,o}A_o\left([\overline{MX_3}]_o - [\overline{MX_3}]_{oi}\right) = k_{MX_3,m}A_{lm}\left([\overline{MX_3}]_{oi}^m - [\overline{MX_3}]_{si}^m\right) = A_i(-R_M)_{si} = k_{M,s}A_i\left([M^{3+}]_{si} - [M^{3+}]_s\right) = \left(\frac{1}{3}\right)k_{H,s}A_i\left([H^+]_s - [H^+]_{si}\right) \quad (8)$$

The continuity of the total flux of the carrier in the stripping module is expressed by

$$K_{(HX)_2}\left([\overline{(HX)_2}]_{si}^m - [\overline{(HX)_2}]_o\right) = 3K_{LaX_3}\left([\overline{LaX_3}]_o - [\overline{LaX_3}]_{si}^m\right) + 3K_{NdX_3}\left([\overline{NdX_3}]_o - [\overline{NdX_3}]_{si}^m\right) \quad (9)$$

The conservation of the PC88A carrier holds in the stripping module if the concentration profiles in membrane and the organic stagnant layer are linear[10,11]:

$$[\overline{(HX)_2}]_0 - [\overline{(HX)_2}]_o = \int\left([\overline{(HX)_2}] + 3\sum[\overline{MX_3}]\right)dx = \left(\frac{1}{2}\right)\left\{[\overline{(HX)_2}]_{si}^m + 2[\overline{(HX)_2}]_{oi}^m + [\overline{(HX)_2}]_{oi} + 3\sum\left([\overline{(MX)_3}]_{si}^m + 2[\overline{(MX)_3}]_{oi}^m + [\overline{(MX)_3}]_{oi}\right)\right\} \quad (10)$$

The two equalities $[\overline{MX_3}]_{oi}^m = [\overline{MX_3}]_{oi}$ and $[\overline{HX_2}]_{oi}^m = [\overline{HX_2}]_{oi}$ are also assumed.

If the mass-transfer coefficients were available, we can calculate all interfacial concentrations of the reactive species by simultaneously solving the set of nonlinear Eqs. 5–10 using the NEQNF program (Fortran version 6.0). The molar fluxes of metals in the extraction module ($J_{M,E}$) and in the stripping module ($J_{M,S}$) are obtained from Eqs. 5 and 8, respectively.

Experimental

Apparatus and solutions

NDSX experiments were conducted using the Hoechst Celanese laboratory system (Model 5PCS-1001; Hoechst Celanese, Charlotte, NC). This module subject to analysis was the Liqui-Cel Extra-Flow 2.5 × 8 cm membrane contactor (Model G261; Hoechst Celanese). It is a small laboratory scale (with two 0–1 dm^3/min pumps and flow meters) that is specifically designed for experimental purposes. Table 2 provides additional information about this module. Figure 3a shows a detailed schematic of the module, which is actually the baffled one where the shell-side fluid flows perpendicular to the fibers.

The extractant PC88A (95% purity; Daihachi Chemical Industry Co., Chuo-ku, Japan) was used as received. Before use, the diluent kerosene (Formosan Union Chemical Corp., Taipei, Taiwan) was washed twice with 20 vol % H_2SO_4 to remove aromatics and then with deionized water (Milli-Q; Millipore, Bedford, MA) three times. The aqueous phase was prepared by dissolving $La(NO_3)_3$ or $Nd(NO_3)_3$ (Merck Co., Darmstadt, Germany) in deionized water, in which the pH was adjusted to be 2–6 by adding a small amount of 100 mol/m^3 of HNO_3 or NaOH. The organic phase was prepared by diluting PC88A with kerosene. The initial (total) concentrations of metals in the aqueous phase and of PC88A dimers in the organic phase ranged from 2 to 24 and from 17 to 137 mol/m^3, respectively. The strip phase consisted of 1 mol/dm^3 of HNO_3. The average densities of feed, organic, and strip phases were 995, 843, and 1095 kg/m^3, respectively, at 25°C. In addition, the average viscosities of feed, organic, and strip phases were 8.94×10^{-4}, 1.09×10^{-3}, and 9.1×10^{-4} kg/(m s), respectively.

Table 2. Characteristics of the Microporous Hollow Fibers Used in This work*

Shell characteristics	
Material	Polypropylene
Length	203 mm
Outer diameter	77 mm
Inner diameter, D_i	63 mm
Hydraulic diameter, d_h	4.7 mm
Fiber characteristics	
Material	Celgard X-30 240 polypropylene hollow fiber
Number of fibers, N	~10,200
Effective length, L	198 mm
Inner diameter, d_i	0.24 mm
Outer diameter, d_o	0.30 mm
Effective surface area	1.4 m^2
Effective area/volume	29.3 cm^2/cm^3
Average pore size, d_p	0.03 μm
Membrane porosity, ε	0.4
Membrane tortuosity, τ	2.6

*Hoechst Celanese Liqui-Cel Extra-Flow 2.5 × 8 cm Membrane Contactor Model G-261.

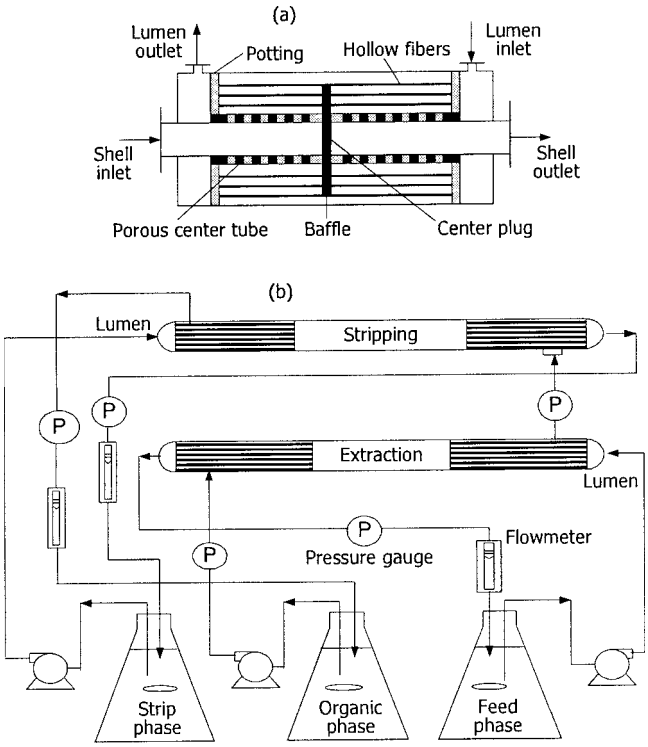

Figure 3. Experimental setup for simultaneous NDSX of metal mixtures in hollow-fiber modules.

NDSX experiments

Figure 3b shows a schematic of the experimental setup. Equal volumes (1 dm^3) of the aqueous and organic phases were pumped through the lumen and shell sides of the modules, respectively, where they came in contact and the mass transfer of metals took place. The temperature was fixed at 25°C. Upon exiting the module, the two streams were totally recycled to each original reservoir. The valves and pressure gauges were used to control the flow rates and to ensure that a positive pressure of 14–35 kPa was maintained on the aqueous side of the module. In this scenario, the aqueous–membrane interface can be stabilized.[16] In commercial-scale countercurrent contacting, the drop in pressure would actually cause one end of the contactor to approach either zero transmembrane pressure difference or a difference that exceeds the breakthrough pressure. This is obviously not a problem with the short module used in this work.

Before the experiments, the organic and metal-free aqueous phases were fed into the module at a flow rate of 6 cm^3/s for 30 min. This flow rate was selected such that both phases could flow steadily. The aqueous phase was then quickly replaced by a metal-bearing solution. At this instance, the experiment was started and samples (2 cm^3) were taken from the aqueous phases at preset time intervals. The dilution effect of the aqueous phase resulting from solution exchange was corrected (roughly 7%). The concentrations of La(III) and Nd(III) in the aqueous phases were analyzed by inductively coupled plasma–optical emission spectrometry (ICP-OES, Optima 2000DV; Perkin Elmer, Norwalk, CT) and those in the organic phase were calculated from a mass balance if necessary. The aqueous pH was measured using a pH meter (Horiba F-23, Kyoto, Japan). Each experiment was at least duplicated under identical conditions. The reproducibility of the concentration measurements was within 5%.

Results and Discussion

Determination of the transport parameters

Here the aqueous flow through the module is laminar (Re < 5). Within this region, the mass-transfer coefficient for the lumen side k_a (k_f or k_s) depends on mean velocity u according to[19]

$$\left(\frac{d_i k_a}{D_j}\right) = 1.62\left(\frac{d_i^2 u_{\text{lumen}}}{D_j L}\right)^{1/3} \tag{11}$$

For the shell side (organic phase), the mass-transfer correlation k_o is[20]

$$\left(\frac{d_h k_o}{D_j}\right) = 5.85(1-\Phi)\left(\frac{d_h}{L}\right)\left(\frac{d_h u_{\text{shell}}}{v}\right)^{0.66}\left(\frac{v}{D_j}\right)^{0.33} \tag{12}$$

where v is the kinematic viscosity of the medium and Φ is the fiber packing density of the module, which equals 0.23 here.[21] This correlation is derived according to NDSX results of various solvents and solutes such as xylene/acetic acid/water and is applicable in the range of $0 < \text{Re} < 500$ and $0.04 < \Phi < 0.4$.[20] Here, d_h is the hydraulic diameter of the shell that is calculated as the cross-sectional flow area divided by the wetted perimeter: $(D_i^2 - \text{Nd}_o^2)/(D_i + N\text{d}_o)$.[21] Under the flow condition studied ($u_{\text{shell}} = 2.9$ mm/s), the calculated k_o value is comparable to that estimated based on the correlations obtained from various flow geometries.[22] It is reasonable to simply assume perfect countercurrent flow on the shell side, although it is the baffled module; that is, the effect of shell-side bypassing of the fibers or shell-side traveling in plug flow is negligible. In fact, Eq. 12 was satisfactorily used in the similar Liqui-Cel 8 × 28 cm 5PCG-259 hollow-fiber module for recovery of gold from aqueous alkaline cyanide solutions.[23]

The diffusion of species through the membrane pores is approximated by diffusion through a cylindrical wall. Thus, the membrane mass-transfer coefficient can be expressed as[16,20]

$$k_m = \frac{2\varepsilon D_j}{\tau(d_o - d_i)} \tag{13}$$

where ε and τ are, respectively, the porosity and tortuosity of the membrane.

Table 1 lists the correlated mass-transfer coefficients. In this correlation, the diffusivities of H^+, Nd^{3+}, and La^{3+} in the aqueous phase are obtained to be 9.3×10^{-9}, 5.7×10^{-10}, and 6.2×10^{-10} m^2/s, respectively, by the Nernst–Hartley equation.[24] The diffusivities of $(HX)_2$, NdX_3, and LaX_3 in the organic phase are calculated by the Hayduk–Minhas equation[25] based on the solution containing 34 mol/m^3 $(HX)_2$. The kinematic viscosity of organic solution was measured to be 8.42×10^{-7} m^2/s at 25°C. On the other hand, the molar volume of kerosene at its normal boiling point is assumed to be the same as that of *n*-dodecane (that is, 278 cm^3/mol).[26] The parachors of kerosene, $(HX)_2$, NdX_3, and LaX_3 are calculated to be 512, 1523, 4522, and 4522 $(cm^3\ g^{1/4})/s^{1/2}$, respectively, by the method of additive group contributions.[25]

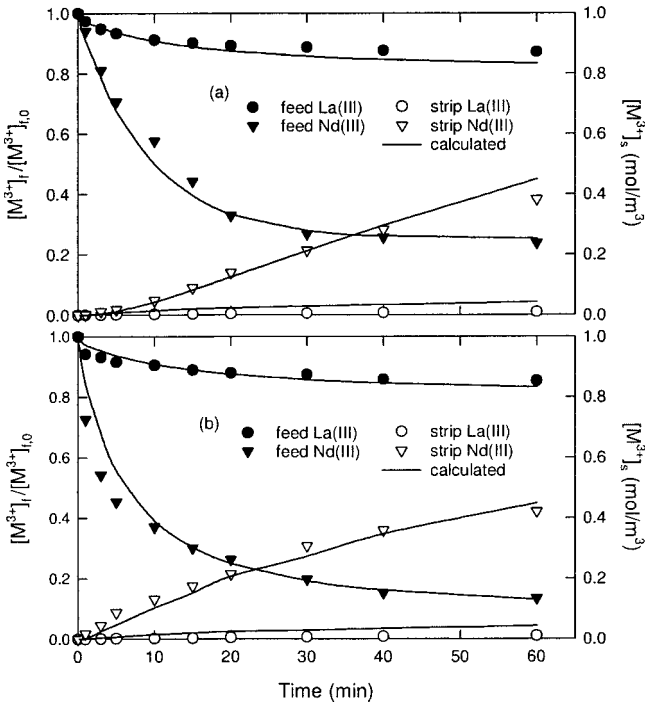

Figure 4. Comparison of the measured and simulated time profiles of aqueous metal concentrations at different feed pH values.

$u_{lumen} = 3.6$ mm/s, $u_{shell} = 2.9$ mm/s, $[La^{3+}]_{f,0} = [Nd^{3+}]_{f,0} = 1.5$ mol/m^3, $[(HX)_2]_0 = 34$ mol/m^3, $[HNO_3]_{s,0} = 1$ mol/dm^3; (a) $pH_{f,0} = 4$ and (b) $pH_{f,0} = 6$.

Comparisons of the simulated and measured results

Figures 4–7 show the measured time profiles of feed- and strip-phase concentrations of binary metals under different conditions. By comparing the ratio of $[Nd^{3+}]/[La^{3+}]$ in the feed and strip phases after 60-min experiments (termed as $\alpha_{f,60}$ and $\alpha_{s,60}$, respectively) with that in the feed phase at $t = 0$ ($\alpha_{f,0}$), we can approximately view the separation potential of this NDSX operation. As shown in Table 3, effective separation of Nd(III) over La(III) is achieved in the strip phase (a concentration ratio ≈ 40) under the conditions of high feed pH values and/or low organic PC88A concentrations. In a comparison of the $\alpha_{f,60}$ and $\alpha_{s,60}$ values as $\alpha_{f,0} = 1$, for example, the separation appears to be contributed primarily by selective stripping. This will be quantitatively discussed below.

In these figures, the solid curves are simulated by simultaneously solving the dynamic mass balances of the following equations[11]:

$$\frac{d[M^{3+}]_f}{dt} = -\left(\frac{1}{V_f}\right) J_{M,E} \tag{14}$$

$$\frac{d[M^{3+}]_s}{dt} = \left(\frac{1}{V_s}\right) J_{M,S} \tag{15}$$

If only a small amount of metals is extracted every time (such as $\Delta t < 1$ s) as the liquids pass through the module, they can be solved numerically by discretization of the equations as follows[17]:

$$[M^{3+}]_{f,t+\Delta t} = [M^{3+}]_{f,t} - \left(\frac{J_{M,E}}{V_f}\right) \Delta t \tag{16}$$

$$[M^{3+}]_{s,t+\Delta t} = [M^{3+}]_{s,t} + \left(\frac{J_{M,S}}{V_s}\right) \Delta t \tag{17}$$

It is noticed that the calculated values of $J_{M,E}$ and $J_{M,S}$ change with time. The time-dependent quantities of $[H^+]_f$ and $[H^+]_s$ are evaluated from the stoichiometric relationships. Close agreement is obtained under the ranges investigated, in which the standard deviation (SD) defined in Eq. 18, is roughly 8%:

$$\mathrm{SD}(\%) = 100 \times \sqrt{\sum_{i=1}^{n} \left(\frac{[M^{3+}]_i^{calc}}{[M^{3+}]_i^{expt}} - 1\right)^2 \Big/ (n-1)} \tag{18}$$

where n represents the number of data points. It is likely that such deviation is mainly a result of the model simplification that k_m remains constant across the entire range of concentrations and, to a lesser extent, arises from the lack of mutual (competitive) effect on binary metal extraction.

An increase in the viscosity of membrane phase during the experiments at high carrier or complex concentrations (attributed to aggregation of the complex) may result in a decrease in k_m.[27,28] Although the determination of transport parameters from correlation equations, just as approached here, is not the best way in the membrane-based processes, direct measurement of some parameters particularly for k_m seems inaccessi-

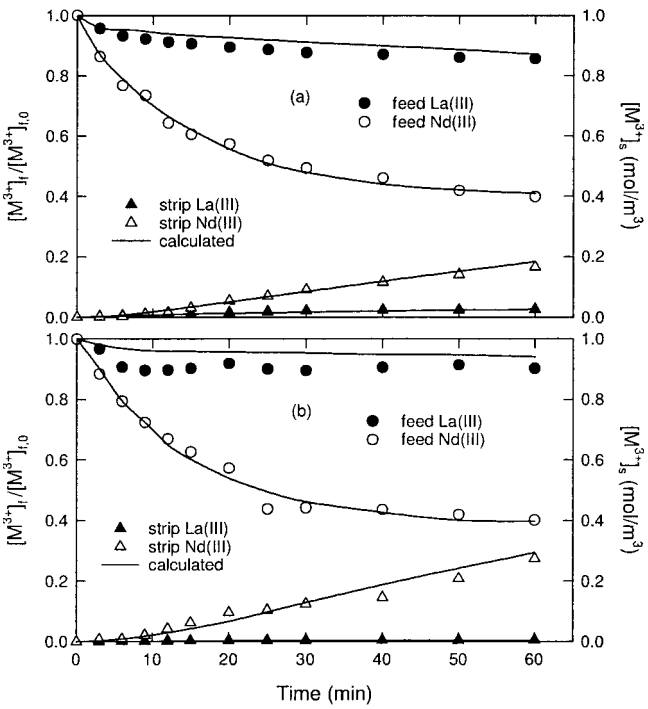

Figure 5. Comparison of the measured and simulated time profiles of aqueous metal concentrations at different concentration ratios.

$u_{lumen} = 3.6$ mm/s, $u_{shell} = 2.9$ mm/s, $pH_{f,0} = 5$, $[(HX)_2]_0 = 17$ mol/m^3, $[HNO_3]_{s,0} = 1$ mol/dm^3; (a) $[La^{3+}]_{f,0} = [Nd^{3+}]_{f,0} = 1$ mol/m^3, and (b) $[La^{3+}]_{f,0} = 0.4$ mol/m^3, $[Nd^{3+}]_{f,0} = 1.6$ mol/m^3.

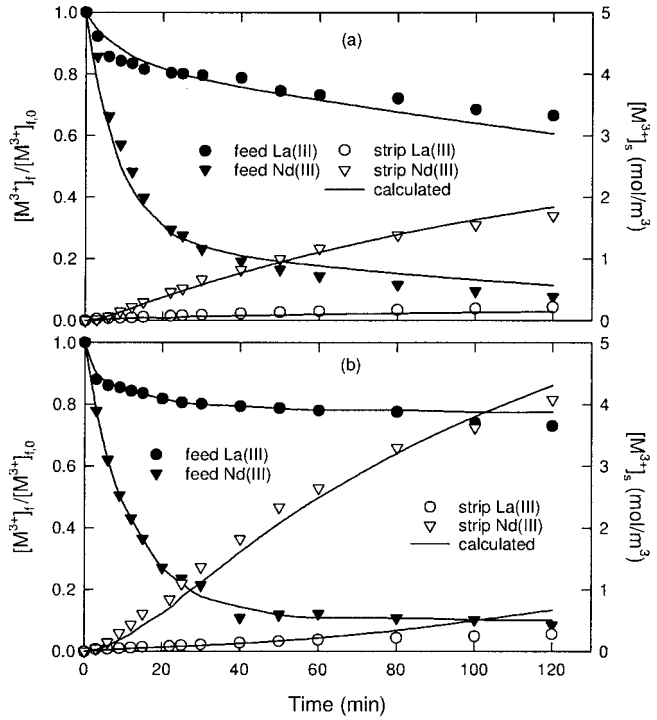

Figure 6. Comparison of the measured and simulated time profiles of aqueous metal concentrations at different total metal concentrations.

u_{lumen} = 3.6 mm/s, u_{shell} = 2.9 mm/s, $pH_{f,0}$ = 6, $[(HX)_2]_0$ = 68.7 mol/m^3, $[HNO_3]_{s,0}$ = 1 mol/dm^3; (a) $[La^{3+}]_{f,0}$ = $[Nd^{3+}]_{f,0}$ = 3 mol/m^3, and (b) $[La^{3+}]_{f,0}$ = $[Nd^{3+}]_{f,0}$ = 12 mol/m^3.

ble. Elhassadi and Do[27] studied the effect of Alamine 336 concentration on the transport of UO_2^{2+} across a supported liquid membrane. They indicated that the viscosity effect is more pronounced in small membrane pores than in SX analogy because the viscosity ratios of the reacted to unreacted carriers calculated from the flux data and measured in the bulk phase are highly inconsistent. In examining the effect of Aliquat 336 concentration on CrO_4^{2-} extraction in hollow-fiber modules [polypropylene (PP), δ = 0.2 mm, d_p = 0.5 μm, ε = 0.63], Alonso et al.[28] also found that the value of k_m for the complex, determined by model fitting of the flux data, decreases from 2.28×10^{-7} to 8.08×10^{-8} m/s when the Aliquat 336 concentration in kerosene increases from 1 to 10% v/v.

As shown above, it is simply assumed that the mass transfer of each metal is independent for modeling NDSX process in binary metal systems; that is, the model parameters obtained in single systems are directly taken. This assumption is likely acceptable when the metal concentration in the aqueous phase is low and PC88A is in substantial excess because in this case the organic loading is low (<12%).[4] Moreover, the extraction of Nd(III) and La(III) has about one-unit difference in their $pH_{1/2}$ values (the pH at which 50% of metals are extracted).[4]

Determination of the mass-transfer mechanisms

To determine the mass-transfer mechanisms, we express $J_{M,E}$ and $J_{M,S}$ in terms of the driving force divided by the sum of all possible resistances. From Eqs. 5 and 8, we have

$$J_{M,E} = K_{M,E}A_i\left([M^{3+}]_f - \frac{[\overline{MX_3}]_o}{m_{M,fi}}\right) \tag{19}$$

$$J_{M,S} = K_{M,S}A_i\left([\overline{MX_3}]_o - m_{M,si}[M^{3+}]_s\right) \tag{20}$$

where $K_{M,E}$ and $K_{M,S}$, the overall mass-transfer coefficients on the basis of each concentration difference shown above, are given by

$$\frac{1}{K_{La,E}} = \frac{1}{k_{La,f}} + \frac{1}{k_{1,La}[\overline{(HX)_2}]_{fi}^{1/2}} + \frac{A_i}{m_{La,fi}A_{lm}k_{LaX_3,m}} + \frac{A_i}{m_{La,fi}A_ok_{LaX_3,o}} \tag{21}$$

$$\frac{1}{K_{La,S}} = \frac{A_i}{k_{LaX_3,o}A_o} + \frac{A_i}{k_{LaX_3,m}A_{lm}} + \frac{[H^+]_{si}^{1/2}}{k_{-1,La}} + \frac{m_{La,si}}{k_{La,s}} \tag{22}$$

$$\frac{1}{K_{Nd,E}} = \frac{1}{k_{Nd,f}} + \frac{1}{k_{1,Nd}[\overline{(HX)_2}]_{fi}} + \frac{A_i}{m_{Nd,fi}A_{lm}k_{NdX_3,m}} + \frac{A_i}{m_{Nd,fi}A_ok_{NdX_3,o}} \tag{23}$$

$$\frac{1}{K_{Nd,S}} = \frac{A_i}{k_{NdX_3,o}A_o} + \frac{A_i}{k_{NdX_3,m}A_{lm}} + \frac{[H^+]_{si}}{k_{-1,Nd}} + \frac{m_{Nd,si}}{k_{Nd,s}} \tag{24}$$

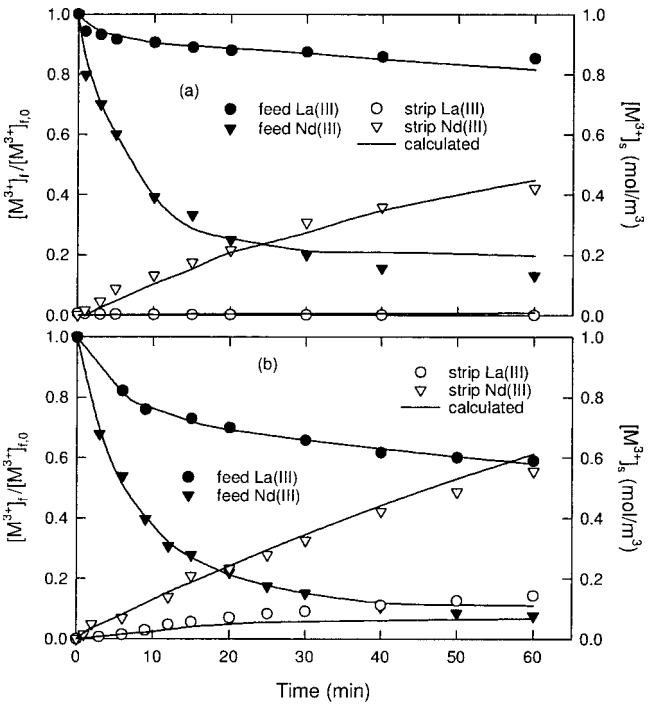

Figure 7. Comparison of the measured and simulated time profiles of aqueous metal concentrations at different PC88A concentrations.

u_{lumen} = 3.6 mm/s, u_{shell} = 2.9 mm/s, $[La^{3+}]_{f,0}$ = $[Nd^{3+}]_{f,0}$ = 1.5 mol/m^3, $pH_{f,0}$ = 5, $[HNO_3]_{s,0}$ = 1 mol/dm^3; (a) $[(HX)_2]_0$ = 34 mol/m^3 and (b) $[(HX)_2]_0$ = 68.7 mol/m^3.

Table 3. Separation Abilities of Nd(III) over La(III) by Batch SX and NDSX with PC88A under Different Conditions ($[HNO_3]_{s,0}$ = 1 mol/dm^3)

$[La^{3+}]_{f,0}$ (mol/m^3)	$[Nd^{3+}]_{f,0}$ (mol/m^3)	$pH_{f,0}$	$[(HX)_2]_0$ (mol/m^3)	$\alpha_{f,0}$	$\alpha^*_{f,60}$	$\alpha_{s,60}$	β^{**}_{SX}	β_{NDSX}
1.5	1.5	2	34	1	0.69	11.9	10.3	7.6
		4		1	0.27	38.0	7.8	7.4
		6		1	0.16	38.5	7.8	7.3
1.6	0.4	5	17	0.25	0.19	3.1	1.2	3.8
1.0	1.0			1	0.47	5.7	8.3	7.6
0.4	1.6			4	0.57	10.5	13.1	10.4
1.5	1.5	6	68.7	1	0.15	4.6	5.8	5.3
3.0	3.0			1	0.19	7.8	7.4	7.2
6.0	6.0			1	0.37	9.9	8.9	12.9
12.0	12.0			1	0.58	12.8	9.2	18.4
1.5	1.5	5	34	1	0.17	38.5	7.8	7.4
			68.7	1	0.21	4.6	5.8	5.1
			137	1	0.23	1.8	3.3	2.9

*$\alpha_{f,1}$, for example, denotes the ratio of $[Nd^{3+}]/[La^{3+}]$ in the feed phase at time t (in minutes).
**Data calculated from Eq. 30 and the mass balances as if SX were performed in the batch mode[4].

Here, either $m_{M,fi}$ or $m_{M,si}$ is a measure of the distribution of metals at the aqueous–membrane (organic) interface, expressed as

$$m_{La,fi} = k_{1,La}[H^+]_{fi}^{1/2}[\overline{(HX)_2}]_{fi}^{1/2} \Big/ k_{-1,La} \quad (25)$$

$$m_{La,si} = k_{1,La}[H^+]_{si}^{1/2}[\overline{(HX)_2}]_{si}^{1/2} \Big/ k_{-1,La} \quad (26)$$

$$m_{Nd,fi} = k_{1,Nd}[H^+]_{fi}[\overline{(HX)_2}]_{fi} \Big/ k_{-1,Nd} \quad (27)$$

$$m_{Nd,si} = k_{1,Nd}[H^+]_{si}[\overline{(HX)_2}]_{si} \Big/ k_{-1,Nd} \quad (28)$$

Because $m_{M,fi}$ and $m_{M,si}$ depend on the initial conditions and operating time, they should be solved first. The four terms in the right-hand side of Eqs. 21–24 represent the resistance of each mass-transfer step. In Eq. 21, for example, they are in order the resistances of aqueous feed-layer diffusion (R_{feed}), chemical reaction (R_{chem}), membrane diffusion (R_{mem}), and organic layer diffusion (R_{org}), respectively. The fractional resistance of each step (Δ_{feed}, Δ_{chem}, etc.) to the overall NDSX process can thus be calculated; for example, Δ_{feed} is given by

$$\Delta_{feed} = \frac{R_{feed}}{(R_{feed} + R_{chem} + R_{mem} + R_{org})} \quad (29)$$

The results calculated in the extraction and stripping modules at $t = 0$ are listed in Tables 4 and 5, respectively. By comparing them, we can quantitatively identify the rate-controlling step(s). It is found that the extraction process is predominantly governed by membrane diffusion ($\Delta_{mem} > 0.76$) under the ranges studied, particularly for the case of Nd(III). However, the stripping process is primarily controlled by combined membrane and strip stagnant-layer diffusion ($\Delta_{mem} + \Delta_{strip} > 0.62$), whereas the contribution of strip stagnant-layer diffusion becomes more important at higher PC88A concentrations. Moreover, the interfacial chemical reaction tends to play a certain role merely in the stripping of Nd(III) at low PC88A concentrations.

Because of the lack of literature results in the NDSX of Nd(III) and La(III) by PC88A, a detailed discussion of the mechanisms obtained here is somewhat challenging, and thus the extraction of other metals with PC88A carriers in membrane-based processes is compared. In modeling the permeation of equimolar Co(II) and Ni(II) from nitrate solutions (1–42.5 mol/m^3) by PC88A/*n*-dodecane across a flat-sheet–supported liquid membrane (Teflon®, $\delta = 0.06$ mm, $d_p = 0.1$ μm, $\varepsilon = 0.57$) to a 3-mol/dm^3 HCl strip solution, Matsuyama et al.[29] considered merely the resistances of the diffusion of metals through the feed stagnant layer and the diffusion of PC88A and their metal complexes in the membrane phase; that is, the resistances of interfacial reactions, diffusion of metals and H^+ in the strip stagnant layer, and diffusion of H^+ in the feed stagnant layer were neglected. Jeong et al.[30] also modeled the transport of equimolar Co(II) and Ni(II) from sulfate solu-

Table 4. Fractional Resistances of the NDSX of Binary Nd(III) and La(III) with PC88A in the Extraction Module at t = 0 ($[HNO_3]_{s,0}$ = 1 mol/dm^3)

$[M^{3+}]_{f,0}$ (mol/m^3)	$[(HX)_2]_0$ (mol/m^3)	$pH_{f,0}$	La(III)				Nd(III)			
			Δ_{feed}	Δ_{mem}	Δ_{chem}	Δ_{org}	Δ_{feed}	Δ_{mem}	Δ_{chem}	Δ_{org}
0.4	17	5	Nil	0.76	Nil	0.24	Nil	0.92	Nil	0.08
1.5	17	5	Nil	0.76	Nil	0.24	Nil	0.92	Nil	0.08
1.5	34	2	Nil	0.76	Nil	0.24	Nil	0.92	Nil	0.08
1.5	34	4	Nil	0.76	Nil	0.24	Nil	0.92	Nil	0.08
1.5	34	6	Nil	0.76	Nil	0.24	Nil	0.92	Nil	0.08
1.5	68.7	6	Nil	0.76	Nil	0.24	Nil	0.92	Nil	0.08
12	68.7	6	Nil	0.76	Nil	0.24	Nil	0.92	Nil	0.08

Table 5. Fractional Resistances of the NDSX of Binary Nd(III) and La(III) with PC88A in the Stripping Module at $t = 0$ ($pH_{f,0} = 5$)

$[M^{3+}]_{f,0}$ (mol/m^3)	$[(HX)_2]_0$ (mol/m^3)	$[HNO_3]_{s,0}$ (mol/dm^3)	La(III)				Nd(III)			
			Δ_{strip}	Δ_{mem}	Δ_{chem}	Δ_{org}	Δ_{strip}	Δ_{mem}	Δ_{chem}	Δ_{org}
0.4	17	1	0.18	0.50	0.18	0.14	0.38	0.24	0.30	0.08
1.5	17	1	0.17	0.50	0.18	0.15	0.38	0.24	0.30	0.08
1.5	34	1	0.27	0.43	0.16	0.14	0.48	0.20	0.25	0.07
1.5	68.7	1	0.30	0.42	0.15	0.13	0.62	0.17	0.15	0.06
12	68.7	1	0.30	0.42	0.15	0.13	0.62	0.17	0.15	0.06

tions (0.85–85 mol/m^3) through a hollow-fiber–supported liquid membrane (PP, $d_i = 0.024$ mm, $\delta = 0.03$ mm, $\varepsilon = 0.3$) with PC88A (10–50 wt %) in kerosene to a strip phase containing 1.5 mol/dm^3 H_2SO_4. Good agreement on the fluxes was found, although the instantaneous chemical reactions between metals and PC88A were assumed. This is probably attributable to the use of relatively high carrier concentrations [160–820 mol/m^3 $(HX)_2$] in contrast to the present work.

Yang et al.[31] analyzed the simultaneous extraction of Cu(II) and Zn(II) with LIX84 and D2EHPA, respectively, in a module containing two sets of hollow fibers (PP, $d_i = 0.1$ mm, $\delta = 0.025$ mm, $d_p = 0.03$ μm, $\varepsilon = 0.4$). Judging from the effect of species concentration and flow rate on the forward extraction rate, they indicated that the resistances of aqueous layer diffusion, interfacial reaction, and membrane diffusion all affect the extraction process, and the first one plays a major role in the Cu(II)–LIX84 system and the last one in the Zn(II)–-D2EHPA system. Yang and Cussler[32] studied competitive extraction of Cu(II) and Ni(II) with a kerosene solution of D2EHPA (10 v/v%) in hollow-fiber modules (PP, $d_i = 0.41$ mm, $\delta = 0.026$ mm, $d_p = 0.04$ μm, $\varepsilon = 0.35$). They also found that the contribution of interfacial reaction is important only in dilute metal solutions (<40 mg/dm^3).

On the other hand, aqueous layer diffusion is known to be rate controlling at a sufficiently low metal level in a membrane-based transport process using acidic carriers.[10,11,33] For example, Hu and Wiencek[33] indicated that aqueous layer diffusion dominates at very low aqueous-phase flow rate, very low metal concentration, and very high carrier concentration in the extraction of Cu(II) with LIX84/kerosene in hollow-fiber contactors (PP, $\delta = 0.2$ mm, $d_p = 0.2$ μm).

Separation factors

It is of practical interest to compare the separation factors of Nd(III) over La(III) under batch SX equilibrium (β_{SX}) and dynamic NDSX conditions (β_{NDSX}), which are defined as[30,31,34]

$$\beta_{SX} = \frac{\left(\overline{[NdX_3]}/\overline{[LaX_3]}\right)}{\left([Nd^{3+}]_0/[La^{3+}]_0\right)} = \left(\frac{K_{ex,Nd}}{K_{ex,La}}\right) \Big/ \left(\frac{1 + K_{ex,Nd}\overline{[(HX)_2]}^3[H^+]^{-3}}{1 + K_{ex,La}\overline{[(HX)_2]}^3[H^+]^{-3}}\right) \quad (30)$$

$$\beta_{NDSX} = \frac{\left(J_{Nd,E}/J_{La,E}\right)_{t=0}}{\left([Nd^{3+}]_{f,0}/[La^{3+}]_{f,0}\right)} \quad (31)$$

The results are also shown in Table 3. Here, β_{SX} is obtained from Eq. 30 and the mass balances as if the SX were performed in the batch mode.[4] The differences between β_{SX} and β_{NDSX} at given conditions can be considered as a measure of whether the NDSX separation process is equilibrium or kinetics controlled.[34] One observes that there are no substantial differences between β_{SX} and β_{NDSX} values, indicating that the separation in the present NDSX process depends on the individual equilibrium parameters (such as $K_{ex,M}$) rather than the diffusivities of metal–PC88A complexes in the membrane and organic phases. More effective separation of Nd(III) over La(III) is achieved at lower PC88A concentrations and lower feed pH values as shown in Table 3, although the extractability is lower in these cases.

The decreased separation factors β_{NDSX} with increasing PC88A concentrations were also previously reported, for example, in the separation of Co(II) over Ni(II) from equimolar solutions in a flat-sheet–supported liquid membrane[29] and a hollow-fiber–supported liquid membrane.[30] The same trends were also observed in the separation of Zn(II) over Cu(II) by D2EHPA in hollow-fiber modules.[34] This is explained by a compromise between the slightly increased concentrations of the complexes at the feed–membrane interface and the sharply decreased diffusivities of species in the membrane (resulting from the increased viscosity of the organic phase).[30] On the other hand, the increased β_{SX} or β_{NDSX} with increasing total metal concentration is possibly explained by the effect of competitive extraction of binary metals at high organic loadings.[4,34]

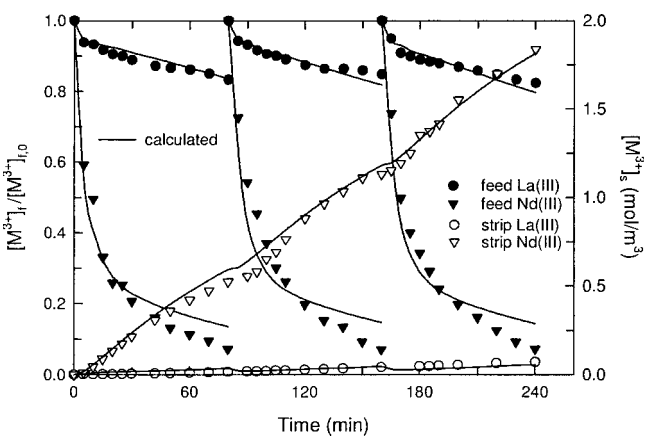

Figure 8. Comparison of the measured and simulated time profiles of aqueous metal concentrations in continuous operations with twice refreshment of feed solution.

$u_{lumen} = 3.6$ mm/s, $u_{shell} = 2.9$ mm/s, $[La^{3+}]_{f,0} = [Nd^{3+}]_{f,0} = 3$ mol/m^3, $pH_{f,0} = 6$, $[(HX)_2]_0 = 68.7$ mol/m^3, $[HNO_3]_{s,0} = 1$ mol/dm^3.

As shown in Table 3, a separation factor of Nd(III) over La(III), in terms of $\alpha_{s,60}$, of nearly 40, is actually obtained at high feed pH and low PC88A concentrations. Comparing the $\alpha_{s,60}$ and β_{NDSX} values, we find that selective stripping of Nd(III) over La(III) from the loaded organic phase plays a crucial role in the present NDSX process. This is an important characteristic of membrane contactors for increasing conversion with the so-called equilibrium-limited chemical reactions.[8] Figure 8 clearly demonstrates the feasibility of the NDSX process for continuous operations with twice refreshment of feed solution. It is also shown that model predictions on time changes of the feed- and strip-phase metal concentrations are satisfactory.

Conclusions

Kinetics and mechanisms of the NDSX separation of Nd(III) over La(III) in two hydrophobic hollow fibers from nitrate solutions with PC88A/kerosene to a HNO_3 solution have been analyzed. A mass-transfer model was proposed that considers all possible resistances involved. On the basis of a good knowledge of extraction chemistry and the transport properties of the relevant geometry, close agreement between the predicted and measured results was obtained (SD, 8%) by directly taking the parameters evaluated in batch SX of single-metal systems. Such a deviation mainly arose from inaccurate estimation of the membrane-phase mass-transfer coefficients.

The proposed method for fractional resistance calculations could give a deeper insight into the mass-transfer mechanism of the NDSX process. Under the conditions studied (total metal concentration 2–24 mol/m^3, feed pH 2–6, dimeric PC88A 17–137 mol/m^3, strip HNO_3 1 mol/dm^3), membrane diffusion controlled the extraction process (fractional resistance $\Delta_{mem} > 0.76$), particularly in the extraction of Nd(III). On the other hand, the stripping process was primarily governed by mixed diffusion in the membrane and strip stagnant layer ($\Delta_{mem} + \Delta_{strip} > 0.62$) and the latter effect was more significant at higher PC88A concentrations. The role of interfacial reaction was important only in the stripping of Nd(III) at low PC88A concentrations. By comparing various types of separation factors ($\alpha_{s,60}$, β_{SX}, β_{NDSX}), we found that the separation of Nd(III) from La(III) by PC88A was essentially equilibrium controlled. However, the NDSX process could improve the separation by selective stripping of Nd(III) from the loaded organic phase at high feed pH and low PC88A concentrations.

Notation

A_i = effective area based on the inner diameter of the fiber, m^2
A_{lm} = effective areas based on the log mean diameter of the fiber, m^2
A_o = effective areas based on the outer diameter of the fiber, m^2
d_h = hydraulic diameter of the shell, m
d_i = inner diameter of the fiber, m
d_{lm} = log mean diameter of the fiber, m
d_o = outer diameter of the fiber, m
d_p = pore diameter of the membrane, μm
D_i = inner diameter of the shell, m
D_j = diffusivity of species j in bulk liquid phase, m^2/s
HX = PC88A monomer
$J_{M,E}, J_{M,S}$ = molar flux in the extraction and stripping modules, respectively, g-mol/s
k_j = individual mass-transfer coefficient of species j, m/s
K_j = overall mass-transfer coefficient of species j defined in Eqs. 19 and 20, m/s
K_{ex} = extraction equilibrium constant defined in Eq. 2
k_1 = forward (extraction) rate constant defined in Eqs. 3 and 4
k_{-1} = backward (stripping) rate constant defined in Eqs. 3 and 4
L = effective length of the fiber, m
$m_{M,fi}$ = distribution ratio of metal at the feed–membrane interface defined in Eqs. 25 and 27
$m_{M,si}$ = distribution ratio of metal at the strip–membrane interface defined in Eqs. 26 and 28
n = number of data points
N = number of fibers
Re = Reynolds number ($=d_i u/\nu$)
R_M = reaction rate of metal extraction with PC88A defined in Eq. 3 or 4, g-mol/(m^2 s)
t = time, s
u = flow velocity, m/s
V = volume of the solution, m^3
$[\overline{V}]$ = concentration of species in brackets, g-mol/m^3

Greek letters

$\alpha_{f,t}$ = molar concentration ratio of Nd(III) to La(III) in the feed phase at time t, min
$\alpha_{s,t}$ = molar concentration ratio of Nd(III) to La(III) in the strip phase at time t, min
β = separation factor of Nd(III) over La(III) defined in Eqs. 30 and 31
δ = thickness of the membrane, m
Δ = fractional resistance defined in Eq. 29
ε = porosity of the membrane
ν = kinematic viscosity of the medium, m^2/s
τ = tortuosity of the membrane
Φ = fiber packing density of the shell

Superscript

m = membrane side adjacent to the liquid–membrane interface

Subscripts

f, m, s = feed, membrane, and strip phases, respectively
i = liquid–membrane interface
t = any time t
0 = initial (total)

Acknowledgments

Financial support for this work by the ROC National Science Council under Grant NSC93-2214-E-155-001 is gratefully acknowledged.

Literature Cited

1. Zhang P, Yokoyama T, Itabashi O, Wakui Y, Suzuki TM, Inoue K. Hydrometallurgical process for recovery of metal values from spent nickel-metal hydride secondary batteries. *Hydrometallurgy*. 1998;50:61–75.
2. Tzanetakis N, Scott K. Recycling of nickel-metal hydride batteries. I. Dissolution and solvent extraction of metals. *J Chem Technol Biotechnol*. 2004;79:919–926.
3. Ritcey GM. Commercial processes for nickel and cobalt. In: Lo TC, Baird MHI, Hanson C, eds. Handbook of Solvent Extraction. New York: Wiley;1983:673–687.
4. Kao HC, Yen PS, Juang RS. Solvent extraction of La(III) and Nd(III) from nitrate solution with 2-ethylhexylphosphonic acid mono-2-ethylhexyl ester. *Chem Eng J*. 2006;119:97–104.
5. Laddha GS, Degaleesan TE. Dispersion and coalescence. In: Lo TC, Baird MHI, Hanson C, eds. Handbook of Solvent Extraction. New York: Wiley;1983:125–149.
6. Bart HJ, Schoneberger A. Reactive processes for recovery of heavy metals in miniplants. *Chem Eng Technol*. 2000;23:653–660.
7. Prasad R, Sirkar KK. Membrane-based solvent extraction. In: Ho WSW, Sirkar KK, eds. Membrane Handbook. New York: Van Nostrand Reinhold;1992:727–763.
8. Gabelman A, Hwang ST. Hollow fiber membrane contactors. *J Membr Sci*. 1999;159:61–106.

9. Bocquent S, Gasscons VF, Muvdi NC, Sanchez J, Athes V, Souchon I. Membrane-based solvent extraction of aroma compounds: Choice of the configurations of hollow fiber modules based on experiments and simulation. *J Membr Sci*. 2006;281:358–368.
10. de Haan AB, Bartels PV, de Graauw J. Extraction of metals from wastewater: Modeling of mass transfer in a supported liquid membrane process. *J Membr Sci*. 1989;45:281–297.
11. Plucinski P, Nitsch W. Calculation of permeation rates through supported liquid membranes based on the kinetics of liquid–liquid extraction. *J Membr Sci*. 1988;39:43–59.
12. Boaudot A, Floury J, Smorenburg HE. Liquid–liquid extraction of aroma compounds with hollow fiber contactor. *AIChE J*. 2001;47: 1780–1793.
13. Soidenhoff K, Shamieh MM. Liquid–liquid extraction of cobalt with hollow fiber contactor. *J Membr Sci*. 2005;252:183–194.
14. Nakashio F, Kondo K, Murakami A, Akiyoshi Y. Extraction equilibria of copper and zinc with alkylphosphonic acid monoester. *J Chem Eng Jpn*. 1982;15:274–279.
15. Laidler KJ, Meiser JH, Sanctuary BC. Physical Chemistry. 4th Edition. Boston, MA:Houghton Mifflin; 2003:429–431.
16. Kiani A, Bhave RR, Sirkar KK. Solvent extraction with immobilized interfaces in a microporous hydrophobic membrane. *J Membr Sci*. 1984; 20:125–145.
17. Koekemoer LR, Buys J, Rollings JE. Use of supported liquid membranes for sulfate extraction from acidic wastewaters. *Sep Sci Technol*. 2000;35:1233–1245.
18. Harrington PJ, Stevens GW. Steady-state mass transfer and modeling in hollow fiber liquid membranes. *J Membr Sci*. 2001;192:83–98.
19. Smith JM, Stammers E, Janssen LPBM. Physical Transport Phenomena I. Delft, The Netherlands:Delft Univ. Press; 1981:91–92,106.
20. Prasad R, Sirkar KK. Dispersion-free solvent extraction with microporous hollow fiber modules. *AIChE J*. 1988;34:177–188.
21. Liang TT, Long RL. Corrections to correlations for shell-side mass-transfer coefficients in the hollow-fiber membrane modules. *Ind Eng Chem Res*. 2005;44:7835–7843.
22. Wickramasinghe SR, Semmens MJ, Cussler EL. Mass transfer in various flow fiber geometries. *J Membr Sci*. 1992;69:235–250.
23. Kumar A, Haddad R, Sastre AM. Integrated membrane process for gold recovery from hydrometallurgical solutions. *AIChE J*. 2001;47: 328–340.
24. Horvath AL. Handbook of Aqueous Electrolyte Solutions: Physical Properties, Estimation and Correlation Methods. New York:Ellis Horwood; 1985:263–298.
25. Reid RC, Prausnitz JM, Poling BE. The Properties of Gases and Liquids. 4th Edition. New York: McGraw-Hill;1987:598–606.
26. Schotte W. Prediction of the molar volume at the normal boiling point. *Chem Eng J*. 1992;48:167–172.
27. Elhassadi AA, Do DD. Effects of a carrier and its diluent on the transport of metals across supported liquid membrane. II. Viscosity effect. *Sep Sci Technol*. 1986;21:285–297.
28. Alonso AI, Irabien A, Ortiz MI. Non-dispersive extraction of Cr(VI) with Aliquat 336: Influence of carrier concentration. *Sep Sci Technol*. 1996;31:271–282.
29. Matsuyama H, Katayama Y, Kojima A, Washijima I, Miyake Y, Teramoto M. Permeation rate and selectivity in the separation of cobalt and nickel by supported liquid membranes. *J Chem Eng Jpn*. 1987;20: 213–220.
30. Jeong J, Lee JC, Kim W. Modeling on the counteractive facilitated transport of Co in Co–Ni mixtures by hollow-fiber supported liquid membrane. *Sep Sci Technol*. 2003;38:499–517.
31. Yang ZF, Guha AK, Sirkar KK. Novel membrane-based synergistic metal extraction and recovery processes. *Ind Eng Chem Res*. 1996;35: 1383–1394.
32. Yang CF, Cussler EL. Reactive dependent extraction of copper and nickel using hollow fibers. *J Membr Sci*. 2000;166:229–238.
33. Hu SB, Wiencek JM. Emulsion-liquid-membrane extraction of copper using a hollow-fiber contactor. *AIChE J*. 1998;44:570–581.
34. Juang RS, Huang HL. Modeling of non-dispersive extraction of binary Zn(II) and Cu(II) with D2EHPA in hollow fiber devices. *J Membr Sci*. 2002;208:31–38.

Manuscript received Apr. 16, 2006, and revision received Dec. 5, 2006.